TESTING AERIAL TRIANGULATION ACCURACY FOR TWO STRIPS OF UAV IMAGES

Amr M. Elsheshtawy[1*], Larisa A. Gavrilova[2],
Anatoly N. Limonov[2],Vasily I. Nilipovskiy[2]

[1] Al-Azhar University, **Egypt**
[2] State University of Land Use Planning, **Russia**

ABSTRACT

In the light of the technological development, small-format camera have been introduced with a photogrammetry technology that offers numerous benefits. The digital imagery by small-format camera installed on a lightweight platform, such as Unmanaged Aerial Vehicles (UAVs), can potentially be applied to produce digital maps. The geometry of the Georeferenced Digital Surface Model (DSM), obtained from UAVs, is as a consequence of a multitude of factors such as flight configuration, camera performance, camera calibration, and Structure from Motion (SfM) algorithms. The overlap percentages among images, the number of images and strips covering the area of interest are important factors in flight planning and estimating the acquisition time. This research have as the main aims to find a way to reduce time length for the acquisition of images as well as for data

---

processing by investigating the effect on georeferencing accuracy of the reduction in the sidelap percentage for two strips of UAV images.

Keywords: UAV, linear projects, overlap, georeferencing, accuracy assessment

INTRODUCTION

UAVs are used in many applications, including land and crop monitoring, surveillance and maintenance of roads, cultural heritage registration and documentation (Tahar and Ahmad, 2012). The impact of the distribution of Ground Control Points (GCPs) in traditional platforms on the spatial quality of orthomosaics was discussed (Wang et al. 2012). The GCPs are not standardized for UAVs and their distribution was analyzed by Carvajal (2016). It was noticed that GCPs came in a range of sizes, from four to over a hundred, and were used to cover areas up to 50 hectares (Agüera et al. 2015; Zhang et al. 2011). Ref. also analyses the accuracy of having less GCPs for the UAV orthomosaics with a Root Mean Square Error (RMSE) of more than one meter. The effect of the images overlap can be divided into two sections: the front overlap and the side overlap (sidelap or lateral overlap). Although the front overlap can be achieved by taking multiple images per second, the lateral overlap is an important variable for the planning of the drone's flight path. There is no well-defined, benchmarked, or tested influence of the side overlaps on Forest landscape restoration (Zhang et al. 2011). The balance between accuracy and efficiency, compensated by time and cost and inherent in all terrestrial and airborne inventories, can be traced back to these trade-offs. Although these exchanges have a clear nature, there is a clear lack of scientific empirical studies that explore space, sensor, and imaging parameters and the available results does not provide the whole range of necessary information on how to optimize the UAV missions. It is thus not surprising that the study of the best image overlap and altitude is becoming increasingly popular (Yuan et al.

146

2009; Snavely et al. 2006). The objective of this experiment is to reduce the time-consuming during flaying in the field and data analysis in the office by studying the influence of decreasing the sidelap percentage from 80% to 60% on georeferencing accuracy.

MATERIALS AND METHODS

Aerial imagery was carried out using DJI Mavic PRO UAV (Figure 1). A three- image strips were taken using DJI Mavic PRO, and during flight a total number of 152 images were obtained. Flight lines were 900 meters in length and the flight altitude was at 60 meters. The spatial resolution was 2 cm at the ground level. The study used 34 ground-points to use as GCPs or checkpoints (CPs), evenly distributed as groups throughout the study area. Each group consisted of about three GCPs and the groups were distributed every 50-100 meters in the length direction of the project (900 m). The distances between points in each group of GCPs were about 20 meters in the width direction (90 m) of the study area as shown in Figure 2. Camera calibration parameters are presented in Table 1. RTK-GNSS, Trimble R4 dual-frequency GPS receivers were used to collect GCPs coordinates. The photogrammetric software Agisoft PhotoScan Professional was used for the photogrammetric data processing.

Figure 1 - DJI Mavic PRO.

Figure 2 - The study area.

Table 1- Camera calibration parameters

Camera Name	FC220 (4.73mm)
Focal length	4.73mm
Resolution	Width = 4000 pixels
	pixel width = 0.0016 mm
	Height = 3000pixels
	pixel width = 0.0016 mm
Principal Distance	c = 4.6501 mm
Principal Point Offsets	xp = 0.0305 mm
	yp = 0.0165 mm
Coefficients of Radial Distortion	K_1 = -8.31719e-004
	K_2 = -3.16310e-005
	K_3 = 3.91019e-006
Coefficients of Decentering Distortion	P_1 = 3.06539e-005
	P_2 = 1.40033e-004

148

Photogrammetric data processing was executed with the commercial software package - PhotoScan (PS), by Agisoft LLC, St. Petersburg, Russia. Block orientation is performed with SfM algorithms in an arbitrary reference frame.

The study was carried out at the GORNOYE scientific and educational base of the State University of Land Use Planning, located in the south of the Moscow Region. The imagery area is 900 m x 90 m.

The multiple groups of tests for studying the influence of using different percentages of side lap between two strips on georeferencing accuracy are shown in table 3. In different groups of tests, different numbers of GCPs were used, and the others were used as CPs to use in the accuracy assessment as shown in Figure 3.

From Table 2 and Figure 3 it can be noticed that the direct georeferencing technique (group A) used only data of camera stations positions given by drone GPS for georeferencing and all thirty-four ground points were used as CPs. On the other hand, the indirect georeferencing technique (group E) used all thirty-four GCPs in georeferencing, and groups B, C, and D used some ground points as GCPs and the other as CPs. In group B three GCPs were used with a bad distribution that was located on one edge of the study area while six and twelve GCPs in groups C and D were used in georeferencing with a good distribution that was covered all projects.

The methodology of this work consisted in studying the influence of decreasing the time of images data acquisition in the field by decreasing the side lap from 80% to 60% between two strips. This allows covering a bigger area of imaging from the two strips. Therefore, the five groups of the test-parameters were designed to test the accuracy of georeferencing resulting when having 60% and respectively 80% side lap between two adjacent strips in each group.

Table 2 - The multiple groups of tests

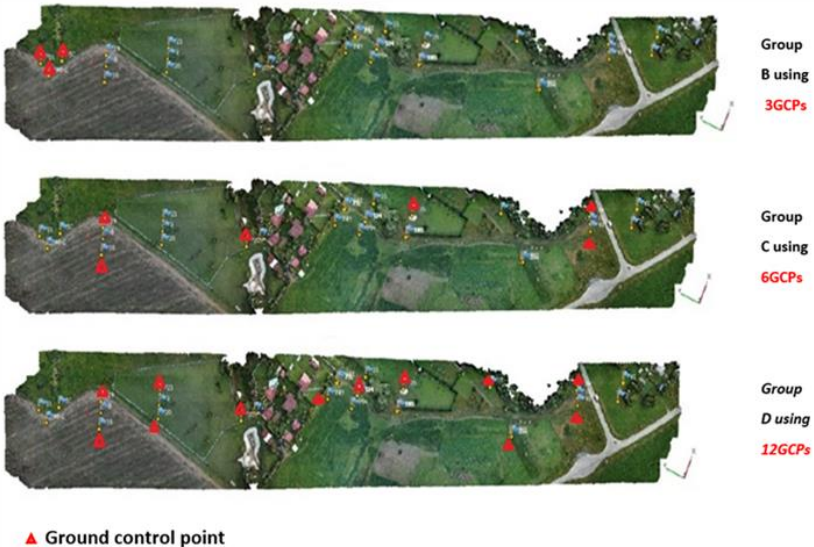| Sections	Group ID	Numbers of GCPs	Sidelap percentage	Test ID	Remarks
First	A	0	60%	0 GCPs 60%	Direct georeferencing
			80%	0 GCPs 80%	
	B	3	60%	3 GCPs 60%	Bad GCPs distribution
			80%	3 GCPs 80%	
Second	C	6	60%	6 GCPs 60%	Well GCPs distribution
			80%	6 GCPs 80%	
	D	12	60%	12 GCPs 60%	Well GCPs distribution
			80%	12 GCPs 80%	
	E	34	60%	34 GCPs 60%	Using all GCPs
			80%	34 GCPs 80%	

▲ Ground control point

Figure 3 - The distribution of GCPs in the study area in the tests of groups B, C, and D.

The test - groups are also divided into two categories, the first one (groups A and B) depending on auxiliary data only or mostly for georeferencing. Direct georeferencing technique (group A) or indirect georeferencing technique (group B) with little support of three GCPs to auxiliary data because of bad distribution and a small number of considered GCPs. The second category (groups C, D, and E) depending on auxiliary data and significant support of GCPs in georeferencing having good distribution and high number of GCPs.

The accuracy assessment was done using the residuals of checkpoints as follows:

When Mx, is RMSE of X, My is RMSE of Y, and Mz (*Vertical Error*) is RMSE of Z. Therefore,

$$Horizontal\ Error = \sqrt{(Mx)^2 + (My)^2} \qquad (1)$$

Total Error is the whole RMSE for X, Y, and Z was calculated as follows.

$$Total\ Error = \sqrt{(Mx)^2 + (My)^2 + (Mz)^2} \qquad (2)$$

RESULTS AND DISCUSSION

The first tests were based on auxiliary data only without the use of any GCPs (Group A) in georeferencing or often on auxiliary data and the assistance of three GCPs in georeferencing (group B). Figures 4 and 5 demonstrate the georeferencing accuracy of the 60% and 80% side lap ratio in Group A tests.

Direct georeferencing technique for test group A showed that the horizontal, vertical and total errors when having 80% sidelap are lower than those obtained when having 60% sidelap (Figure 4). In tests performed on group B 3 GCPs were used to help georeferencing. In this case, the vertical and total error of the 80% sidelap is lower than the results obtained for 60%. In contrast, the horizontal error for the 80% side lap test is greater than resulting in the case of 60%, as shown in Figure 5. In the first section of the test groups although most variations between the test errors

are not significant, 80% sidelap tests often provided lower error values than tests with a 60% side lap between the test strips.
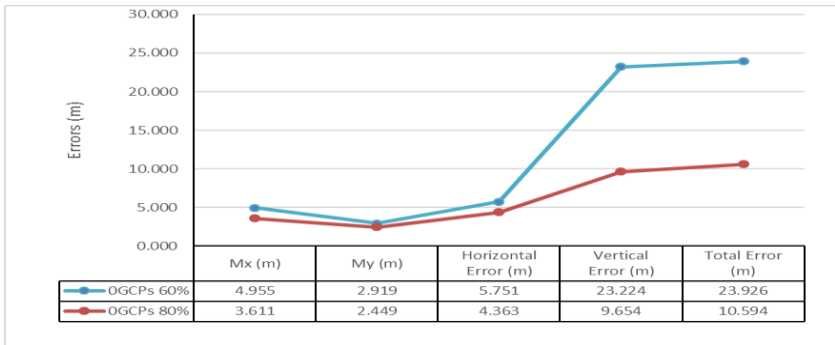

	Mx (m)	My (m)	Horizontal Error (m)	Vertical Error (m)	Total Error (m)
0GCPs 60%	4.955	2.919	5.751	23.224	23.926
0GCPs 80%	3.611	2.449	4.363	9.654	10.594

Figure 4 - The errors of checkpoints without using any GCPs in georeferencing.

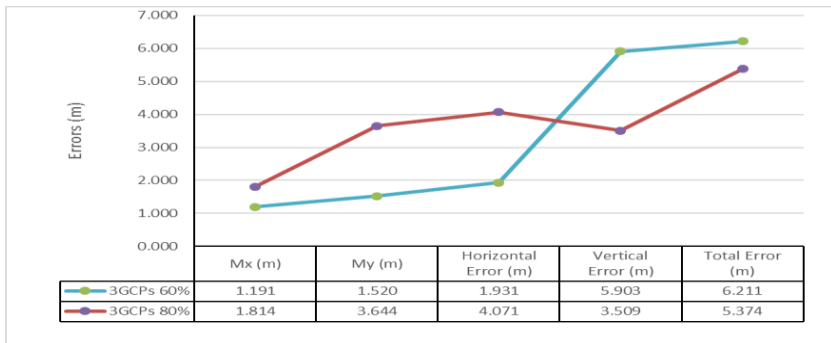|	Mx (m)	My (m)	Horizontal Error (m)	Vertical Error (m)	Total Error (m)
3GCPs 60%	1.191	1.520	1.931	5.903	6.211
3GCPs 80%	1.814	3.644	4.071	3.509	5.374

Figure 5 - The errors of checkpoints when using 3 GCPs in georeferencing.

The second section of tests (groups C, D, and E) mainly depends on GCPs to assist Aero-Triangulation. Figures 6, 7, and 8 demonstrate the georeferencing accuracy of the 60% and 80 % side lap ratio.
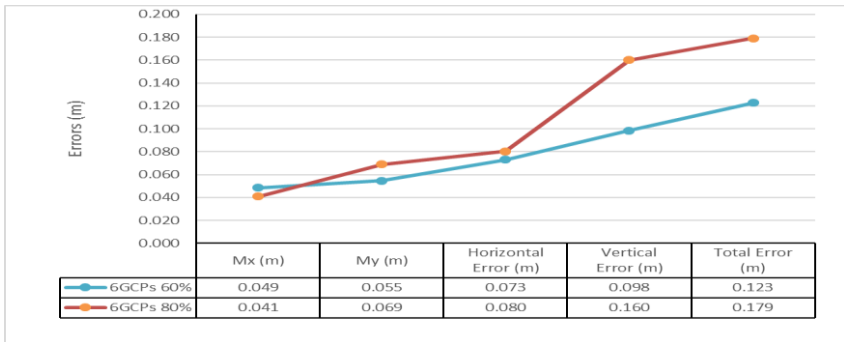
	Mx (m)	My (m)	Horizontal Error (m)	Vertical Error (m)	Total Error (m)
6GCPs 60%	0.049	0.055	0.073	0.098	0.123
6GCPs 80%	0.041	0.069	0.080	0.160	0.179

Figure 6 - The errors of checkpoints when using 6 GCPs in georeferencing.

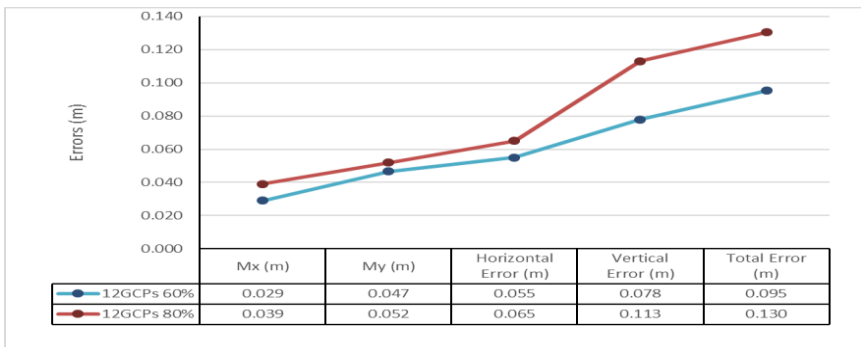|	Mx (m)	My (m)	Horizontal Error (m)	Vertical Error (m)	Total Error (m)
12GCPs 60%	0.029	0.047	0.055	0.078	0.095
12GCPs 80%	0.039	0.052	0.065	0.113	0.130

Figure 7 - The errors of checkpoints when using 12 GCPs in georeferencing.

In the direct georeferencing technique, as applied for groups C, D, and E tests, the horizontal, vertical and total errors of 60% sidelap tests proved to be lower than those obtained when having 80% sidelap, as shown in Figures 6, 7, and 8. In the second section of the test groups, although most variations between the test errors are very small and are not significant, the 60% sidelap tests results are showing lower error values than obtained in tests when used an 80% side lap between the test strips.
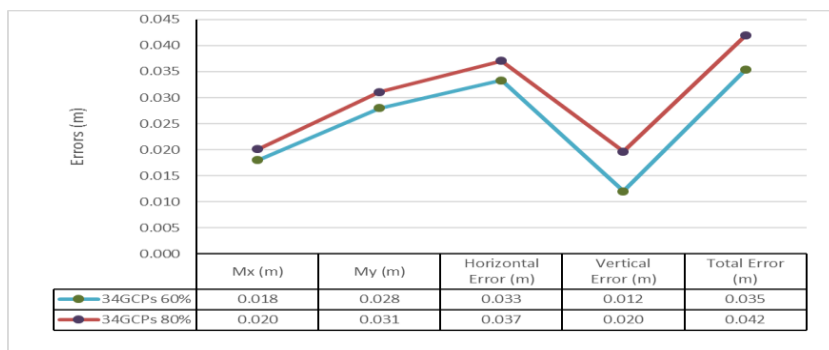
153

	Mx (m)	My (m)	Horizontal Error (m)	Vertical Error (m)	Total Error (m)
34GCPs 60%	0.018	0.028	0.033	0.012	0.035
34GCPs 80%	0.020	0.031	0.037	0.020	0.042

Figure 8 - The errors of checkpoints when using 34 GCPs in georeferencing.

CONCLUSIONS

The significant effect on many aspects, including time and cost of work, make determining the optimal image overlap and altitude appealing. Just before UAVs are imaging linear projects with a length much greater than their width (road projects, electrical installations, piping, and other linear infrastructure projects), the side lap ratio between strips has a significant impact on the time and cost of the work. Consequently, this research covered various tests related to the study of the effect on georeferencing accuracy of reducing the side lap percentage from 80% to 60 %. From the above results and their analysis it can be noticed that there were no significant differences between higher or lower sidelap percentages. Moreover, the accuracy of indirect georeferencing technique tests that have appropriate amounts and distributions of GCPs with lower sidelap is a little better than the georeferencing tests with higher sidelap percentages. For reducing time consumption during the acquisition of images it is recommended to use two strips 60 percent sidelap that will cover a bigger area of imaging more than 80 percent sidelap. In addition, the low number of images for the same region should reduce the processing time.

REFERENCES

Agüera F., Carvajal F., Pérez M., Orgaz F., 2015, Multi-temporal imaging using an unmanned aerial vehicle for monitoring a sunflower crop. Biosyst. Eng. 132, 19–27.

Carvajal F., Agüera F., Martínez P.J., 2016, Effects of image orientation and GCP distribution on unmanned aerial vehicle photogrammetry projects on a road cut slope. J. Appl. Remote Sens., in press.

Küng O., Strecha C., Beyeler A., Zufferey J.-C, Floreano D., Fua P., Gervais F., 2011, The accuracy of automatic photogrammetric techniques on ultra-light UAV imagery. In Proceedings of the UAV-g 2011-Unmanned Aerial Vehicle in Geomatics, Zürich, Switzerland, 14–16 September.

Snavely N., Seitz S.M., Szeliski R., 2006, Photo tourism: Exploring photo collections in 3D. ACM Trans. Graph. 25, 835–846.

Tahar K. N., Ahmad A., 2012, A simulation study on the capabilities of rotor-wing unmanned aerial vehicles in aerial terrain mapping International J. Appl. Phys. Vol. 7(8), 1300 – 1306

Wang J. Ge.Y., Heuvelink G.B.M., Zhou C., Brus D., 2012, Effect of the sampling design of ground control points on the geometric correction of remotely sensed imagery. Int. J. Appl. Earth Observ. Geoinf. 18, 91–100.

Yuan X., Fu J., Sun H., Toth C., 2009, The application of GPS precise point positioning technology in aerial triangulation. ISPRS J. Photogramm. Remote Sens. 64, 541–550.

Zhang Y., Xiong J., Hao L., 2011, Photogrammetric processing of low-altitude images acquired by unpiloted aerial vehicles. Photogramm. Rec. 26, 190–211.